Available online at www.sciencedirect.com
SCIENCE DIRECT®
Carbohydrate Research 338 (2003) 1771–1785
CARBOHYDRATE RESEARCH
www.elsevier.com/locate/carres

Dilute liquid crystals used to enhance residual dipolar couplings may alter conformational equilibrium in oligosaccharides

Patrick Berthault,[a] Damien Jeannerat,[b] Franck Camerel,[c] Francisco Alvarez Salgado,[a,d] Yves Boulard,[d] Jean-Christophe P. Gabriel,[c,e] Hervé Desvaux[a,*]

[a] *Laboratoire Commun de R.M.N., DSM/DRECAM/Service de Chimie Moléculaire, URA 331 CNRS, C.E.A./Saclay, F-91191 Gif sur Yvette, France*
[b] *Département de Chimie Organique, Université de Genève, 30 quai Ernest Ansermet, CH-1211 Genève, Switzerland*
[c] *Sciences Moléculaires aux Interfaces, FRE 2068 CNRS, 2 rue de la Houssinière, B.P. 32229, F-44322 Nantes, France*
[d] *Laboratoire Commun de R.M.N., DSV/DBJC/Service de Biochimie et de Génétique Moléculaire, C.E.A./Saclay, F-91191 Gif sur Yvette, France*
[e] *Nanomix Inc., 5980 Horton Street, Sixth floor, Emeryville, CA 94608, USA*

Received 14 October 2002; received in revised form 20 February 2003; accepted 17 May 2003

Abstract

The solution structures of a trisaccharide and a pentasaccharide containing the Lewis^x motif were determined by two independent approaches using either dipolar cross-relaxation (NOE) or residual dipolar coupling (RDC) data. For the latter, one-bond $^{13}C-^{1}H$ RDC enhanced by two different mineral liquid crystals were used alone. Home-written programs were employed firstly for measuring accurately the coupling constants in the direct dimension of non-decoupled HSQC experiments, secondly for transforming each RDC data set into geometrical restraints. In this second program, the complete molecular structure was expressed in a unique frame where the alignment tensor is diagonal. Assuming that the pyranose rings are rigid, their relative orientation is defined by optimizing the glycosidic torsion angles. For the trisaccharide, a good agreement was observed between the results of both approaches (NOE and RDC). In contrast, for the pentasaccharide, strong discrepancies appeared, which seem to result from interactions between the pentasaccharide and the mesogens, affecting conformational equilibrium. This observation is of importance, as it reveals that using simultaneously NOE and RDC can be hazardous as the former represent 99% of the molecules free in solution, whereas the latter correspond to less than 1% of the structure bound to the mesogen.

Keywords: Residual dipolar coupling; Lewis^x; Mineral liquid crystal; Oligosaccharide; Conformer equilibrium

1. Introduction

Residual dipolar couplings (RDC) enhanced by dilute liquid crystals are recognized as valuable tools for the structure determination of biomolecules through NMR spectroscopy.[1,2] The small degree of anisotropy introduced in the molecular motion leads to non vanishing dipolar interactions and therefore, to supplementary experimental data referenced to the same external frame. The prerequisite is that the 3D structure of the molecule under study is not affected by the presence of the mesogen. Even if only a small fraction of molecules (typically 10^{-3}–10^{-4}) interacts with the mesogen, there is no direct and general proof that the average structure in solution, as determined from dipolar cross-relaxation experiments (NOE), is the same as the one given by RDC. Indeed classical NMR data, such as chemical shifts or relaxation times measured in oriented media and compared to isotropic values cannot answer to this question, since the extracted values cannot figure out the few hundredths of a percent of the molecule bound to the mesogen.

The situation may worsen when structures of small flexible compounds are studied, since: (i) most of the atoms are close to the surface and then potentially interact with the mesogen; (ii) the presence of the mesophase can displace the equilibrium between the conformers. This effect has already been directly detected for small organic compounds dissolved in chiral

* Corresponding author. Tel.: +33-169-086483; fax: +33-169-089806.
E-mail address: hdesvaux@cea.fr (H. Desvaux).

0008-6215/03/$ - see front matter © 2003 Elsevier Ltd. All rights reserved.
doi:10.1016/S0008-6215(03)00243-X

liquid crystals[3] or deduced for flexible parts of large biomolecules.[4] Despite these concerns, the use of RDC has risen hopes for oligosaccharides, since they can efficiently complete the NOE and scalar *J*-coupling data, too scarce to allow safe determination of their conformation in solution.[5,6] However, as outlined by Neubauer and coworkers[7], only a few one-bond C–H RDC non isotropically distributed—due to the geometry of the pyranose rings—can be used. Additional H–H RDC could reinforce these data, but at the price of: (i) larger uncertainty due to cross-relaxation between the coherences leading to the different lines of the multiplets; (ii) more time-consuming measurements; and (iii) not straightforward processing. Indeed, conversely to one-bond C–H RDC, for which it can be assumed that their values only depend of the orientation of the associated bond vector (the bond length is, in first approximation, considered as constant), the H–H RDC have to be translated into inter-proton distances and orientations. Moreover, the presence of internal dynamics of the proton pair under investigation strongly complicates the processing. This explains why many authors only use one-bond C–H RDC as complements of NOE and scalar *J*-coupling data.[6,8]

It is therefore expected that the future importance of the RDC data in the solution structure refinement of oligosaccharides will be determined not only by their versatility, both for the experimental measurement and their translation into geometrical restraints, but also by the insurance that the structure of the molecule under study is not altered by the presence of the nearby mesogen. Assessing the validity of the structures directly derived from one-bond ^{13}C–^{1}H RDC requires using a procedure which can transform pure orientational data into structural restraints. We have developed such a procedure and used it on oligosaccharides in which the number of degrees of freedom defining the structure is strongly limited (two dihedral angles per glycosidic bond). The structures derived by this procedure can then be directly compared to those determined from NOE only. For the RDC data, we have used two different mineral liquid crystals,[9] whose most interesting properties reside firstly in the low material required to induce alignment (1–3% compared to 5–30% for bicelles), and secondly in the absence of ^{1}H, ^{13}C, or ^{15}N NMR signals from the mesogens, facilitating the study of unlabelled molecules.[10] These mineral liquid crystals are an aqueous suspension of V_2O_5[11] and a lamellar phase composed of covalent rigid planes of $H_3Sb_3P_2O_{14}$ dispersed in water.[12] We have considered two compounds belonging to the blood group determinant family: a trisaccharide **1** and a pentasaccharide **2** (Fig. 1). Both oligosaccharides are chosen for the Lewis^x motif, known to be rigid (Gal-β-(1→4)-[Fuc-α-(1→3)]-GlcNAc). Thanks to this choice the internal motions of this domain are almost identical in **1** and **2**, allowing safe comparison of the determined structures. The additional presence in the pentasaccharide **2** of a sulfated group in position 3 of the Gal unit of the Lewis^x and of a more flexible domain composed of the last two units Gal-β-(1→4)-Glc leads to dramatic consequences on the RDCs data of the Lewis^x domain, since they can no longer be represented by a unique alignment tensor. This seems to be due to a conformational exchange around the GlcNAc–Gal glycosidic bond which is modified by the nearby presence of the mesogens.

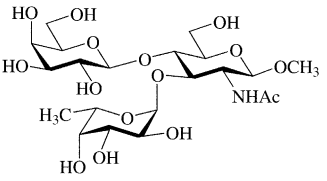

1

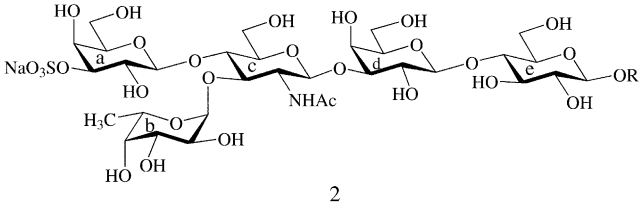

2

Fig. 1. Chemical structures of the trisaccharide **1** and the pentasaccharide **2** (R = CH_3). It contains the sulfated Lewis^x motif and a more flexible domain constituted by the lactose part.

2. Results and discussion

2.1. Exploitation of the residual dipolar couplings

2.1.1. Strategy for structure determination based on RDC. Among all the approaches proposed for exploiting RDC in the general case of biomolecules,[13–15] only two have been used for oligosaccharides in the literature:

1) Starting from a template structure determined from NMR or X-ray data, the five parameters of the RDC tensor (its axial D_a and rhombic D_r amplitudes, and the Euler angles α_R, β_R, γ_R defining its orientation) can be extracted from this initial structure. Then using an iterative procedure, the structure is refined against the RDC.[8,16]
2) Well-defined structural domains of a molecule can be positioned through the orientations of their RDC tensors.[7,17] In order to solve the problem of orientational degeneracy, at least two sets of measures in media inducing different orientations are required.[18] Only this second approach enables direct assessment of the RDC data, treating them independently of the NOE.

However, for oligosaccharides, the risk that the mesogens change the structure of the compound is quite serious, since the energy barriers around the glycosidic bonds are small. In the present exploratory study, we have developed a method belonging to the second type of approach. It takes advantage of the following remarks:

- Assuming that a pyranose ring is rigid,[19] the knowledge of its orientation, as defined for instance by the {C-1,H-1,O-1} frame (see Section 5.3.3 and Fig. 2) is sufficient to derive the orientation of any C–H bond of the ring.†
- The orientation of one pyranose ring relative to the next one can be defined using only two internal degrees of freedom (the two glycosidic angles ϕ and ψ). In these conditions, we avoid the use of the three Euler angles[20] required for defining the relative orientation of two different rigid independent elements, as it is done classically.

This approach implies strong requirements on the quality of the RDC data and correct estimation of the uncertainty. It allows us to assess the consistency of the underlying assumptions and of the protocol, and to explore the effect of the interactions between the molecule under study and the mesogens.

2.1.2. Theoretical basis. Let us consider a C–H bond and the associated dipolar coupling in an oriented medium, taken as a perturbation of the Zeeman Hamiltonian. In the frame attached to the C–H bond, the dipolar Hamiltonian is:

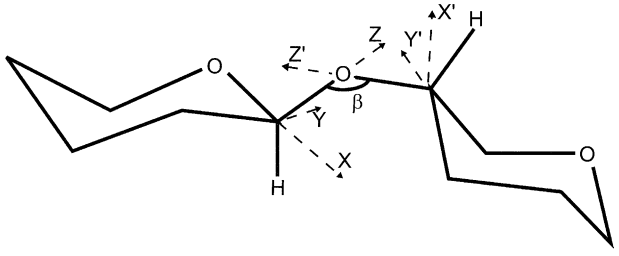

Fig. 2. Frames used to define the orientation of one pyranose ring relative to the next one. The frame named {C-1, H-1, O-1} is defined by the three axes {X,Y,Z}. The second frame {C-4, H-4, O-1} is defined by the three axes {X′, Y′, Z′}. During the computation of RDC, the transformation performed by the numerical procedure used the three Euler angles (α,β,γ). It consists in performing a rotation along the Z′ axis by an angle α (this obviously corresponds to a change on the ψ angle C-1–O-4–O-4–O-3 of the glycosidic bond [21]), followed by a rotation of β around the new Y″ axis, which allows the alignment of the Z′ and Z axes (this rotation corresponds to the bond angle C-1–O-1–O-4) and finally a rotation of γ along the Z axis (γ is obviously related to the ϕ angle O-5–C-1–O-4–C-4 [21]).

$$H_D = \zeta A_{20} T_{20}, \tag{1}$$

where ζ is the normalization coefficient, A_{20} is the nuclear spin operator and T_{20} is the second rank tensor representing the spatial degrees of freedom. This Hamiltonian can be expressed in the frame where the alignment tensor is diagonal:[20]

$$H_D = \zeta A_{20} \sum_{m=-2}^{2} D^2_{m0}(\alpha,\ \beta,\ \gamma) T_{2m}. \tag{2}$$

The second rank tensors T_{2m} are now expressed in this new frame. D^2_{mn} are the second rank Wigner matrices, and α, β, γ are the three Euler angles describing the change of frame. They only depend on the molecular structure and are consequently constant if the structure is assumed to be rigid. Taking a weighted average over all directions the molecule can take:[22]

$$\begin{aligned}[H_D] &= \zeta A_{20}(D^2_{00}(\alpha,\ \beta,\ \gamma)[T_{20}] + D^2_{20}(\alpha,\ \beta,\ \gamma)\\ &\quad [T_{22}] + D^2_{-20}(\alpha,\ \beta,\ \gamma)[T_{2-2}]) = A_{20}(D_a D^2_{00}(\alpha,\ \beta,\ \gamma)\\ &\quad + D_r(D^2_{20}(\alpha,\ \beta,\ \gamma) + D^2_{-20}(\alpha,\ \beta,\ \gamma))) \end{aligned} \tag{3}$$

$$= \left(D_a \frac{3\cos^2\beta - 1}{2} + \sqrt{\frac{3}{2}} D_r \sin^2\beta \cos 2\alpha\right)(\mathbf{IS} - 3I_z S_z). \tag{4}$$

This expression is similar to the classical one[23] except that the use of Wigner matrices slightly changes the coefficients. The new definitions of D_a and D_r induce the boundary condition for rhombicity: $|D_r/D_a| < 1/\sqrt{6}$.[24]

The latter equation can be generalized to take into account any number of rotations by describing them with Wigner matrices. For instance, assuming a rigid molecule and considering two successive changes of molecular frame and the third frame being the frame where the alignment tensor is diagonal, we obtain after averaging along the direction of the alignment tensor:

$$\begin{aligned}[H_D] &= D_a(\mathbf{IS} - 3I_z S_z)\\ &\quad \times \sum_{m,n} D^2_{m0}(\alpha,\ \beta,\ \gamma) D^2_{nm}(\alpha',\ \beta',\ \gamma') D^2_{0n}(\alpha_R,\ \beta_R,\ \gamma_R)\\ &+ D_r(\mathbf{IS} - 3I_z S_z) \sum_{m,n,p} D^2_{m0}(\alpha,\ \beta,\ \gamma) D^2_{nm}(\alpha',\ \beta',\ \gamma')\\ &\quad \times [D^2_{2n}(\alpha_R,\ \beta_R,\ \gamma_R) + D^2_{-2n}(\alpha_R,\ \beta_R,\ \gamma_R)], \end{aligned} \tag{5}$$

where the different sets of Euler angles correspond to the successive changes of frame. The inherent advantages of this approach are the following:

† The reciprocity is not true since, for particular structures and taking into account a finite precision on the RDC measurements, the number of directions effectively sampled by the C–H bonds can be reduced to about two (all C–H bonds in axial position) per pyranose ring.

- The Euler angles defining the relative orientations of all C–H bonds inside rigid regions are perfectly known. This can help choosing a judicious frame.
- The orientation of one rigid part relative to another one is expressed in the minimum number of internal degrees of freedom.[25] For instance, by defining the change of frame along a glycosidic bond, Fig. 2, only the α and γ Euler angles vary, while β is constant and equal to the glycosidic bond angle.
- In the case of internal flexibility, and as soon as it could be assumed that the overall average on the orientation of the alignment tensor can be separated from the internal degrees of freedom, (see Section 4) a local order parameter can be introduced.[26] Depending on the number of RDC measurements and their associated accuracies, its determination can be possible.

2.2. Solution structure from dipolar cross-relaxation measurements

For medium size compounds, distances between protons cannot be safely extracted from NOESY experiments, as the size of the molecule causes the NOE to almost vanish and to be strongly dependent on the local internal dynamics. To circumvent this difficulty and to reduce the angular dispersion and the Hartmann–Hahn coherence transfers present in on-resonance ROESY, we have decided to use off-resonance ROESY.[27,28]

For the trisaccharide **1**, due to the rigidity of the Lewis^x motif,[29] we have mainly exploited a magnetization build-up curve from off-resonance ROESY experiments at an angle ϑ between the static and effective fields equal to 54.7° and mixing times between 50 and 300 ms. Twenty NOE restraints were extracted and used in a simulated annealing procedure, leading to 36 accepted structures out of 50, based on energy criteria and the absence of proton–proton distance violations.

For the pentasaccharide **2**, by varying the angle ϑ , the longitudinal and transverse cross-relaxation rates (Eq 7) were determined and the internuclear distances were derived through a procedure which takes into account the local dynamics variations.[29] The 44 H–H distances thus extracted were used as distance restraints in a simulated annealing procedure, leading to 37 structures based on the same criteria of acceptance. The root mean square deviation to the average structure was 0.9 Å considering the non-hydrogen atoms, and 0.55 Å when only the 'backbone' atoms (C-1, C-2, C-3, C-4, C-5, C-6, O-5) were taken into account. These values were 0.52 and 0.13 Å for the trisaccharide **1**, confirming the rigidity of the Lewis^x motif. However, a simulation made for the trisaccharide confirmed that the NOE suffered from bad sampling. As an example, a variation of the Gal-H-1–GlcNAc-H-4 distance from 2.1 to 2.9 Å led to variation of the Gal/GlcNAc dihedral ϕ angle from 300 to 321° and of the Gal/GlcNAc ψ angle from 124 to 138°, for almost the same number of accepted structures.

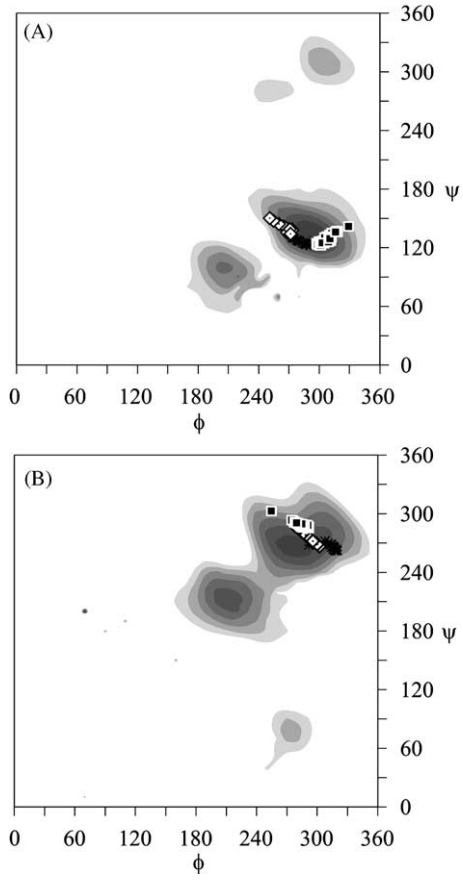

Fig. 3. ϕ-ψ Energy map for the Gal/GlcNAc bond (A) and the Fuc/GlcNAc bond (B) of the trisaccharide **1**. Black squares: results obtained by the NOE approach, black asterisks: results using procedure a form RDC measured in V_2O_5, white diamonds: RDC measured in $H_3Sb_3P_2O_{14}$. For the NOE, due to an uncertainty on the GalH1-GlcNAcH4 cross-peak intensity (strong spectral overlap), the resulting ϕ-ψ values given here arise from different sumulated annealings performed with this distance varied from 2.1Å to 2.9Å.

For both oligosaccharides, the ϕ and ψ glycosidic angles were found in the lowest energy region of the maps computed by molecular modelling.(Figs. 3 and 4, Tables 1 and 2). The average ϕ and ψ values were in agreement with those reported for similar Lewis^x motifs.[8,16,30–37]

2.3. Measurements of RDC in two mineral liquid crystals

The first orienting medium consisted of a D_2O suspension of vanadium pentoxide ribbons at 2.3% w/w, and the second one of a suspension of covalent planes composed of $H_3Sb_3P_2O_{14}$ dispersed in D_2O at 3% w/w. Both are known to form a monodomain at room temperature in the presence of a magnetic field.[12,38]

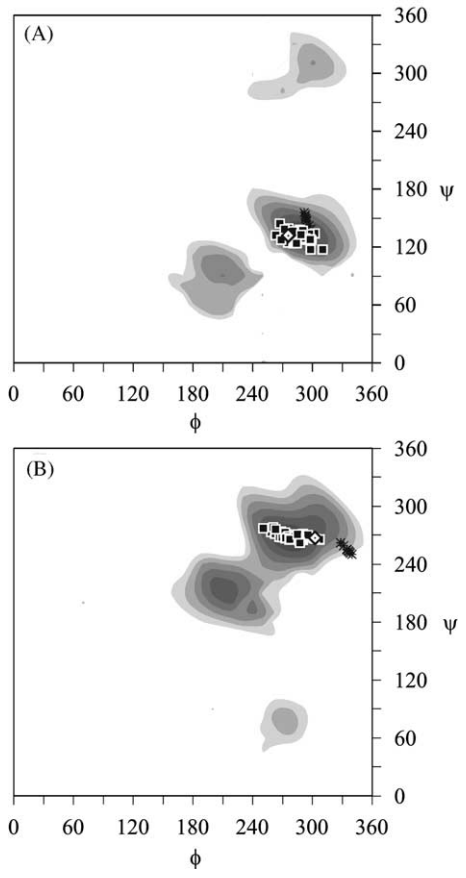

Fig. 4. ϕ-ψ Energy map for the Gal/GlcNAc bond (A) and the Fuc/GlcNAc bond (B) of the pentasaccharide **2**. The same pictographic codes as in Fig. 3 are used.

For both systems, the one-bond $^{13}C-^{1}H$ RDC of **1** and of **2** were measured by comparing the heteronuclear couplings in the proton dimension of non-decoupled HSQC experiments with sensitivity enhanced by gradients,[39] to the equivalent couplings measured by the same pulse sequence in the isotropic phase. In order to obtain the molecular structure only from RDC data, a good accuracy in their measurement and a realistic estimation of their uncertainties was needed. The absence of decoupling during acquisition does not induce more peak overlap than with decoupling, and thus the use of the IPAP type approaches[40,41] is not required. Detecting the splitting in the carbon dimension is obviously less dependent on the remote dipole–dipole proton interactions, but nevertheless suffers from the low digital resolution in this dimension, from the larger efficiency of proton–proton NOE and from the more efficient cross-relaxation between the two lines of the doublet.[42] Using a pulse sequence in which the cross-peak intensities are linked to the splitting could be biased by systematic deviation[43] or would require the fit of an extra parameter.[44] In contrast, the precision of a measurement in the direct dimension was studied long time ago for a single peak.[45] As the two cross-peaks have similar linewidth in the 2D experiment, we have decided to develop a deconvolution program to increase the precision of the measurement relative to direct peak-picking (see Section 5.2.3).

2.4. Solution structures from RDC measurements

2.4.1. Procedure a. The optimal glycosidic dihedral angles were derived for the four sets of RDC obtained in the two orienting media and for both oligosaccharides **1** and **2**. Starting from a template structure, a first estimation of the three Euler angles (α_R, β_R, γ_R) defining the alignment tensor was computed. Then two angle sets, the first one composed of the four glycosidic torsion angles of the Lewis^x motif and the second one composed of the three Euler angles (α_R, β_R, γ_R) were iteratively optimized through a self-consistent procedure (Fig. 5).

For both oligosaccharides, the glycosidic angles fall into low-energy regions (Figs. 3 and 4). In Tables 1 and 2, the average ϕ and ψ values and the associated standard deviations are given. The latter are strongly correlated to the estimation of the uncertainties of the RDC measurements. For instance, for **1** in V_2O_5, the

Table 1
Average glycosidic $\phi-\psi$ angles in degrees and axial and rhombic components of the RDC tensor D_a-D_r in Hz with the standard deviation (superscript) as determined by the different methods (using either NOE or RDC) for the trisaccharide **1**

Method	Gal/GlcNAc		Fuc/GlcNAc							
	ϕ	ψ	ϕ	ψ	α_R	β_R	γ_R	D_a	D_r	χ^2
NOE	$308^{(10)}$	$129^{(10)}$	$284^{(10)}$	$289^{(10)}$	–	–	–	–	–	
$H_3Sb_3P_2O_{14}$	$266^{(5)}$	$141^{(7)}$	$290^{(8)}$	$277^{(7)}$	71.1	59.3	348.0	$-43.3^{(1.1)}$	$-10.6^{(1.1)}$	10.8
V_2O_5	$280^{(4)}$	$128^{(5)}$	$314^{(6)}$	$266^{(3)}$	78.7	47.6	127.3	$-92.9^{(1.5)}$	$-24.3^{(0.9)}$	26.4
$H_3Sb_3P_2O_{14}$	$288^{(3)}$	$138^{(11)}$	$287^{(1)}$	$280^{(3)}$	$55^{(7)}$	$61.2^{(0.5)}$	$345^{(3)}$	$-42.4^{(0.2)}$	$-12.1^{(1.6)}$	9.9
V_2O_5	$281^{(3)}$	$128^{(5)}$	$319^{(4)}$	$262^{(6)}$	$82^{(3)}$	$47.3^{(0.8)}$	$122.6^{(0.6)}$	$-89.9^{(0.7)}$	$-25.9^{(0.9)}$	25.4

For each liquid crystalline medium, the first set (rows 2 and 3) corresponds to the minimization with α_R, β_R, and γ_R kept constant (Section 2.4.1). In the second set (rows 4 and 5), these angles were simultaneously refined with the $\phi-\psi$ angles (Section 2.4.2). The average final χ^2 values are given in the last column.

Table 2
Average glycosidic ϕ–ψ angles in degrees and axial and rhombic components of the RDC tensor D_a–D_r in Hz with the standard deviation (superscript) as determined by the different methods (NOE or RDC approaches) for the pentasaccharide **2**

Method	Gal/GlcNAc		Fuc/GlcNAc							
	ϕ	ψ	ϕ	ψ	α_R	β_R	γ_R	D_a	D_r	χ^2
NOE	$286^{(11)}$	$131^{(6)}$	$279^{(12)}$	$269^{(4)}$	–	–	–	–	–	
$H_3Sb_3P_2O_{14}$	$275.8^{(0.1)}$	$132.2^{(0.4)}$	$302.5^{(0.2)}$	$266.9^{(0.1)}$	133.9	30.4	311.3	$-9.4^{(0.5)}$	$-3.2^{(0.7)}$	12.1
V_2O_5	$294^{(5)}$	$149^{(2)}$	$335^{(3)}$	$254^{(4)}$	66.3	55.3	136.5	$-25.4^{(0.9)}$	$-0.9^{(0.6)}$	14.4
$H_3Sb_3P_2O_{14}$	$356^{(7)}$	$96^{(7)}$	$314^{(8)}$	$43^{(3)}$	$30^{(2)}$	$83^{(2)}$	$132.7^{(0.2)}$	$26.5^{(0.5)}$	$7.9^{(0.9)}$	3.5
V_2O_5	$296^{(4)}$	$126^{(9)}$	$338^{(6)}$	$315^{(10)}$	$5^{(7)}$	$81^{(2)}$	$122^{(2)}$	$-17.4^{(0.7)}$	$-5.1^{(0.3)}$	6.8

For each liquid crystalline medium, the first set (rows 2 and 3) corresponds to the minimization with α_R, β_R and γ_R kept constant (Section 2.4.1). In the second set (rows 4 and 5), these angles were simultaneously refined with the ϕ–ψ angles (Section 2.4.2). The average final χ^2 values are given in the last column.

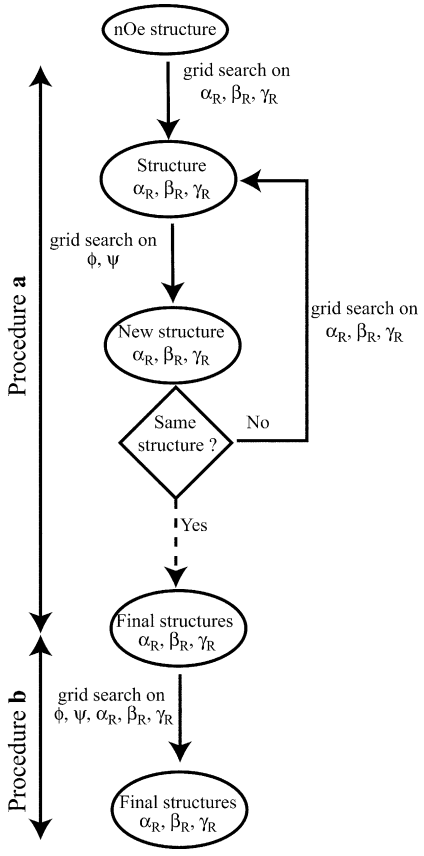

Fig. 5. Numerical procedures **a** and **b** used to determine the structure of the oligosacharides from RDC. For each solid arrow, each set of angles defines a geometry allowing the determination of the D_a and D_r coefficients by linear least-square fitting to the experimental RDC. In procedure **a**, the grid search is performed successively and iteratively on the torsional angles (ϕ, ψ) and on the molecular frame orientation (α_R, β_R, γ_R). In procedure **b**, the grid search is simultaneously performed on all angles.

average ϕ value of the Fuc/GlcNAc glycosidic bond is about 309° instead of 314°, when the uncertainties on the RDC values of GlcNAc C-1–H-1 and C-5–H-5 are increased (these resonance lines partially overlap in both dimensions). Nevertheless, the standard deviations on the ϕ and ψ values are always small, revealing the intrinsic coherence of our experimental data.

Comparison of the alignment tensor parameters (last two columns of Tables 1 and 2) already reveals the much larger order parameter for the trisaccharide than for the pentasaccharide (about a factor 4 in D_a for the same mesogen concentration). This striking result was confirmed by the observation of the RDC for a mixture of the two oligosaccharides dissolved in an aqueous suspension of vanadium pentoxide (Fig. 6). Concerning the Euler angles α_R, β_R and γ_R, referenced to the same frame {Fuc C-1, Fuc H-1, GlcNAc O-3}, the values in columns 5–7 of Tables 1 and 2 show that the alignment induced by the aqueous suspensions of V_2O_5 and $H_3Sb_3P_2O_{14}$ are different, but more surprisingly that the orientation of the dipolar coupling tensors induced by V_2O_5 for **1** and **2** are almost parallel (about 70, 50, 130° for α, β_R, γ_R); only their magnitudes differ.

In contrast to the case of the trisaccharide **1**, the average values of the ϕ–ψ angles found for **2** are different for both liquid crystalline media, and can even be considered as significantly different on a statistical point of view (rows 2 and 3 of Table 2). As this is not observed for **1**, it could result either from uncertainties on the RDC or from incompatible measurements arising from interactions between the mesogen and the molecule.

2.4.2. Procedure b. In a second step, the four glycosidic angles of the Lewis^x motif and the three Euler angles (α_R, β_R, γ_R) were simultaneously minimized (Fig. 5). Here again the situation is different for the oligosaccharides. For **1**, the minima were found close to the initial solutions and they correspond to realistic torsion angles (Table 1, rows 4 and 5). For **2**, the minimization always converged to values far away from the initial values given by procedure **a**. These ϕ, ψ angles were located in well-defined regions of the energy maps

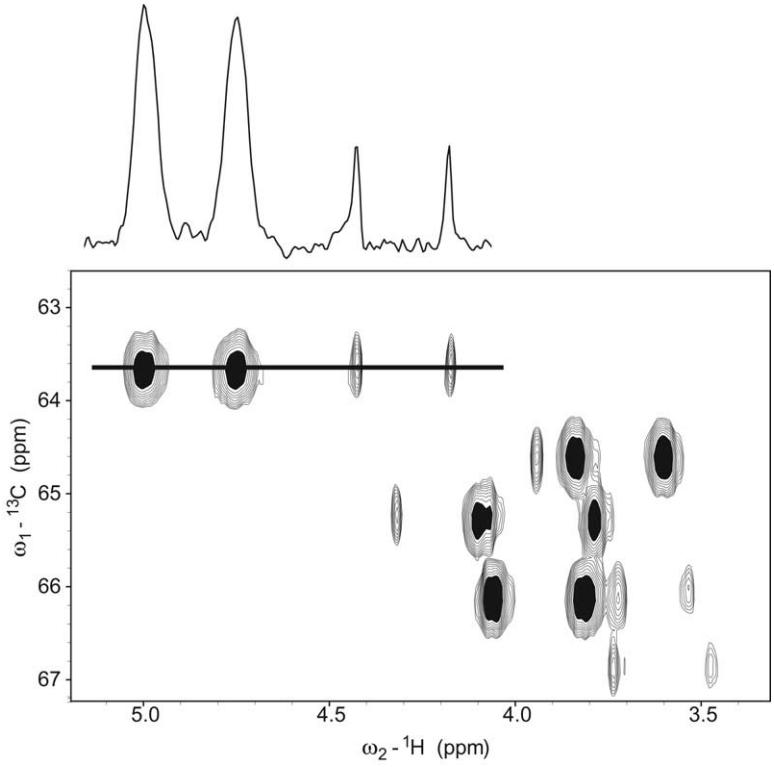

Fig. 6. Sub-spectrum of a 2D HSQC experiment without decoupling during acquisition. The sample was composed of a mixture of the trisaccharide **1** and the pentasaccharide **2** dissolved in an aqueous suspension of V_2O_5. The slice at the level of the solid line is presented on top of the 2D spectrum. The filled peaks correspond to the trisaccharide and the unfilled ones to the pentasaccharide. One can notice that the corresponding half-widths are strongly different and cannot be imputed to the difference of concentration. This variation of linewidth results from the unresolved long-range proton-proton dipolar couplings. This clearly shows that the orientation parameter of the trisaccharide is much larger than that of the pentasaccharide. This result is confirmed by the determination of the one-bond ^{13}C-^{1}H residual dipolar couplings.

(Table 2, rows 4 and 5), but the associated structures led to high energy values as soon as van der Waals terms were taken into account (see energy maps in Fig. 7). This surprising result cannot be ascribed to the numerical procedure for the following reasons:

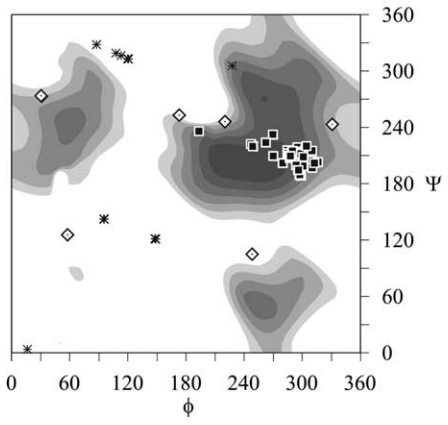

Fig. 7. ϕ-ψ Energy map of the bond between the GlcNac (c) unit and the mono-sulfated galactose (d) unit of the pentasaccharide **2**. The same pictographic code as in Fig. 3 are used.

- If the discrepancy results from lack of convergence due to degeneracy problems in the RDC approach, the same effect would also be present for the Lewis^x motif of the trisaccharide **1**, or for simulated data, where, even using large domains of possible angles and RDC of the same magnitude order as those found for **2**, the program always converges to the right solution. Also, the problem of degeneracy resulting from a particular orientation tensor cannot be invoked, since, as already mentioned, **1** and **2** have the same (α_R, β_R, γ_R) values in V_2O_5 aqueous suspension. In the case of the pentasaccharide and only in that case, starting from a reasonable structure, the program always converges to a very distant solution.
- The lack of convergence in the case of **2** can be due to biased RDC sets. The influence of bad sampling or bad quality of the experimental data on the stability of the program was consequently explored by consistency computations. Systematically 1 out of the 15 RDC values was removed and the complete minimization procedure was performed on this new data set. Similar minima were found without large variation on the χ^2 values. Moreover, the systematic

calculation of the alignment tensor on all sets of data obtained after removing one or two RDC and using a reasonable structure of the Lewis^x motif did not reveal large variations of the RDC tensors nor of the χ^2 values. These results indicate that the experimental data as well as their associated errors are correctly estimated, and that the direction of the tensor is correctly sampled.

As the numerical procedure cannot be incriminated, the discrepancy should originate from the assumptions made, fulfilled for **1** but not for **2**. The three assumptions are that: (i) the pyranose units are rigid; (ii) the internal dynamics (order parameters) is uniform for the Lewis^x motif; and (iii) RDC can be represented by a unique alignment tensor (derivation of Eq (5)). It would be very unlikely that the assumptions (i) and (ii) were not fulfilled for the Lewis^x motif of these two oligosaccharides, given their similarity and the results on internal dynamics obtained by off-resonance ROESY. In contrast, the third assumption of a unique alignment tensor, does not concern a local domain but is affected by the properties of the *whole molecule*. Indeed the relation between the RDC and the molecular frame assumes its existence and its uniqueness. Now, for a molecule exhibiting a conformational equilibrium, a molecular frame should be defined for each conformer. As shown in Section 4, under the key assumption that the presence of the mesogen does not modify the conformational equilibrium, RDC can still be described by an *effective* alignment tensor for a rigid structural element. This assumption is however unrealistic in many cases of small flexible compounds, since the conformational equilibrium results from a balanced effect of internal and solvation interactions. As the alignment of a biomolecule induced by the oriented liquid crystalline media results from the interactions between the mesogen and the biomolecule, its conformational equilibrium should be affected by this supplementary energy term. Even if this effect seems usually not be taken into account in NMR spectroscopy of biomolecules, it has already been reported for small organic compounds dissolved in concentrated liquid crystal media.[3]

Coming back to our experimental systems, there are two main differences between these oligosaccharides **1** and **2**: the presence, in the pentasaccharide, of other organic functions such as the sulfate group and of a more flexible domain constituted by the last two pyranose rings (units (d) and (e)). This might explain the presence of more than one alignment tensor, either generated by competitive interactions between the pentasaccharide and the mesogens or due to different populations of the pentasaccharide conformers. We have explored the importance of the electrostatic interactions with the mesogen involving the sulfate group by measuring RDC in aqueous suspensions of $H_3Sb_3P_2O_{14}$ for a pentasaccharide similar to **2** but without sulfate group on the galactopyranose unit (a) (the molecule studied by Henry and coworkers[35]). Since these measurements reveal an order parameter $S = 2\pi D_a r^3/\gamma_C\gamma_H\hbar$ much smaller than that of the trisaccharide **1**, a Coulombian repulsion with the mesogens cannot be invoked to explain the small order parameter and the discrepancy in the case of the pentasaccharide **2**. This result is comforted by the similarity in (α_R, β_R, γ_R) for the tri- and the pentasaccharide as measured in aqueous suspensions of V_2O_5. The second assumption (modified conformational equilibrium) is finally the only remaining possible explanation to the large variation of the order parameters (factor 4, see Fig. 6), and to the discrepancy in the fitting procedure. Elements can substantiate their presence, even if for **2** the NOE data arising from off-resonance ROESY are compatible with a unique conformation. Indeed conformational exchange around the GlcNAc–Gal glycosidic bond has been observed for similar compounds.[35,37] This chemical exchange obviously affects the whole shape of the pentasaccharide. Finally, since it involves surface pyranose groups, it should be dependent on interactions with mesogens relative to solvation interactions.

3. Conclusions

A numerical method based only on RDC was used for determining the structures of two oligosaccharides containing the Lewis^x motif. This approach takes advantage of the structural features of oligosaccharides (rigid pyranose rings linked by flexible bridges) and of the change of frames made possible by Wigner matrices, to directly deal with the minimal number of internal degrees of freedom. In such a way, through adequate choice of the reference frames, the relative orientation of two pyranose units does only depend on the two glycosidic torsion angles, instead of the three Euler angles when classical changes of frame are considered. This approach has been validated on simulated data and on experimental data on the Lewis^x motif of the trisaccharide. For the latter, correct structures were obtained for all procedures. In contrast, for the *same rigid domain* of the pentasaccharide, surprising results were obtained: (i) order parameter four times smaller than this of the trisaccharide; (ii) structures dependent on the liquid crystal when the parameters of the orientation tensor were kept constant in the minimization (Section 2.4.1); and (iii) non-sense structures, when these parameters were simultaneously optimized with the glycosidic torsion angles (Section 2.4.2). The most likely explanation is that the interactions between the mesogen and the oligosaccharide inducing its alignment change the conformational equilibria in the flexible domain of the pentasaccharide. This result is obviously

embarrassing for the structure determination of oligosaccharides using RDC. If the structure is rigid, the NOE approach is sufficient. If at the contrary the molecule exhibits a high flexibility, then we can be confronted with this modification of the conformational equilibrium.

On a physical point of view, this effect is not surprising since the molecular alignment results from interactions between mesogens and the biomolecule which superimpose and compete with solvation interaction. It is likely that the two energy contributions are different, leading to different populations of conformers. If one considers now large structured biomolecules, for which the core energy becomes the dominating term, it is likely that any conformational exchange affecting a limited region (for instance a flexible loop) cannot largely change the whole alignment tensor, making the approach based on RDC combined to NOE and scalar couplings robust, as illustrated by the large literature in this field. The question however remains open for smaller compounds, such as oligosaccharides. Since the NOE and J-coupling data sample the (e.g., $>99\%$) molecule free in solution, it is only using approaches only based on RDC, as the one used here, that the effect of interactions can be revealed. Even if these studies could appear as purely academical, they seem to us of key importance for assigning a correct weight to the RDC constraints relative to the NOE ones in molecular modelling procedures used for determining solution structures. They correspond also to a nice approach to interpret the physical mechanisms inducing the biomolecule alignment but also to probe the mesogen surface. This last question has to be correlated to the physical explanation of the resulting quadrupolar splitting of D_2O which is only poorly related to the orientation parameter of the liquid crystalline media and of its concentration (see Ref. 38 for an example).

4. Appendix

If we consider a molecule interacting by two or more different manners with the mesogens or exhibiting more than one conformation, and if we assume no interconversion between these conformations when bound to the mesogens, each case can be treated as in Section 2.1.2. The observed splitting is a weighted average over all these cases, and it is not straightforward that, even for a rigid domain, the RDC can be expressed by the classical expression (Eq (4)). We show here that under the key assumption of independent averaging, it always exists a unique *effective* alignment tensor, and therefore angular restraints from RDC can be computed using Eq (4).

Let us assume for the present time that, due to the coexistence of two conformations or two different interactions, the observed RDC are a sum of two contributions. We shall note in the following (α_T, β_T, γ_T) the Euler angles which allow the transformation from the frame R_1, where the first interaction (coefficients D_a^1, D_r^2) is diagonal, to the frame R_2 where the second one (coefficients D_a^2, D_r^2) is diagonal. The orientation of this first alignment tensor relative to the effective one R_e will be described by the Euler angles (α_R, β_R, γ_R). For any C–H bond, whose orientation relative to the frame R_e is defined by the angles α, β, γ, the RDC can be written as:

$$
\begin{aligned}
D \triangleq\ & D_a^{eff} D_{00}^2(\alpha,\ \beta,\ \gamma) \\
& + D_r^{eff}[D_{20}^2(\alpha,\ \beta,\ \gamma) + D_{-20}(\alpha,\ \beta,\ \gamma)] \\
& = D_a^1 \sum_m D_{m0}^2(\alpha,\ \beta,\ \gamma) D_{0m}^2(\alpha_R,\ \beta_R,\ \gamma_R) \\
& + D_r^1 \sum_m D_{m0}^2(\alpha,\ \beta,\ \gamma)[D_{2m}^2(\alpha_R,\ \beta_R,\ \gamma_R) \\
& + D_{-2m}^2(\alpha_R,\ \beta_R,\ \gamma_R)] \\
& + D_a^2 \sum_{m,p} D_{m0}^2(\alpha,\ \beta,\ \gamma) D_{pm}^2(\alpha_R,\ \beta_R,\ \gamma_R) D_{0p}^2(\alpha_T,\ \beta_T,\ \gamma_T) \\
& + D_r^2 \sum_{m,p} D_{m0}^2(\alpha,\ \beta,\ \gamma) D_{pm}^2(\alpha_R,\ \beta_R,\ \gamma_R) \\
& \times [D_{2p}^2(\alpha_T,\ \beta_T,\ \gamma_T) + D_{-2p}^2(\alpha_T,\ \beta_T,\ \gamma_T)]. \qquad (6)
\end{aligned}
$$

If the assumption of the existence of an effective tensor is valid for any C–H bond, Eq (6), should be valid whatever (α, β, γ). Therefore, the coefficients of the five Wigner matrices $D_{m0}^2(\alpha,\ \beta,\ \gamma)$ must vanish. A set of five non-linear equations ($m \in \{-2, 2\}$) with 5 unknowns (D_a^{eff}, D_r^{eff}, α_R, β_R, γ_R) and a condition ($|D_r^{eff}/D_a^{eff}| < 1/\sqrt{6}$) is then derived:

$$
\begin{aligned}
& D_a^{eff}\delta_{0m} + D_r^{eff}[\delta_{-2m} + \delta_{2m}] = D_a^1 D_{0m}^2(\alpha_R,\ \beta_R,\ \gamma_R) \\
& + D_r^1[D_{2m}^2(\alpha_R,\ \beta_R,\ \gamma_R) + D_{-2m}^2(\alpha_R,\ \beta_R,\ \gamma_R)] \\
& + D_a^2 \sum_p D_{pm}^2(\alpha_R,\ \beta_R,\ \gamma_R) D_{0p}^2(\alpha_T,\ \beta_T,\ \gamma_T) \\
& + D_r^2 \sum_p D_{pm}^2(\alpha_R,\ \beta_R,\ \gamma_R) \\
& \quad \times [D_{2p}^2(\alpha_T,\ \beta_T,\ \gamma_T) + D_{-2p}^2(\alpha_T,\ \beta_T,\ \gamma_T)].
\end{aligned}
$$

Existence of solutions of this system has been explored numerically. Values α_R, β_R and γ_R are extracted from the set of three equations composed of the two for which $m = \pm 1$, the third one being obtained by subtracting the equation for $m = -2$ to that with $m = 2$. The coefficients D_a^{eff} and D_r^{eff} are finally computed from the equation for $m = 0$ and $m = 2$, respectively, and the condition $|D_r^{eff}/D_a^{eff}| < 1/\sqrt{6}$ is checked. This exploration, performed on a large number of randomly chosen values of α_T, β_T, γ_T, $D_{a,r}^{1,2}$ reveals that there are always four sets of Euler angles ($\alpha_R, \beta_R, \gamma_R$) fulfilling the conditions. This result being obtained for two alignment

tensors can, by a straightforward generalization, be extended to any number of alignment tensors.

As a conclusion, whatever the conformational space explored by the molecule in the isotropic phase or the existence of different interactions between the molecule and the mesogens, the measurements can always be represented by an *effective* alignment tensor valid for the whole molecule. This result allows the calculation of the RDC in any rigid domain, even in the presence of a flexible one. It seems however useful to stress the assumptions made during this derivation. Indeed during the averaging leading to Eq (4), it is assumed that the angles α, β and γ defining the molecular geometry are *constant*. This means that the extra energy term resulting from the nearby presence of the mesogens should have no influence on the structure of the molecule, or in other words that it *does not promote conformational equilibria.* If this assumption is not valid, one can no more conclude that RDC can be represented by Eq (4) using an effective alignment tensor.

5. Material and methods

5.1. Synthesis

The two saccharides were synthesized by Y. M. Zhang and P. Sinaÿ. The trisaccharide **1** was prepared as described by Yvelin and coworkers.[34] The synthesis of the pentasaccharide **2** is described in a Note in this issue.[46]

5.2. NMR measurements

5.2.1. Sample preparation. Before each preparation, oligosaccharides **1** and **2** were freeze-dried. For the isotropic samples, 2 mg of **2** (5.4 mg of **1**) were dissolved in 400 μL D_2O (99.96% from Eurisotop), resulting in a concentration of 5.2 mM (24.8 mM, respectively). Dealing with pentasaccharide **2**, the second sample was constituted by 0.31 mg of **2** mixed with 400 μL of a D_2O solution of V_2O_5 at 2.34% w/w, synthesized as described by Desvaux and coworkers,[10] leading to a final solute concentration of 0.8 mM. No vigorous shaking or sonication was necessary. For the third sample, 0.6 mg of **2** were dissolved in 250 μL D_2O, and this solution was added to 250 μL of a D_2O solution of $H_3Sb_3P_2O_{14}$ at 3% w/w, which synthesis is described by Gabriel and coworkers.[12] The final solute concentration of **2** was therefore 1.2 mM, and the mineral liquid crystal was at 1.5% w/w. Also no shaking or sonication was necessary. For the liquid crystal solutions containing the trisaccharide, the first one was prepared by dissolving 2 mg of **1** into 400 μL of a D_2O solution of V_2O_5 at 2.34% w/w (final concentration of the trisaccharide: 9.2 mM). The second one was prepared by dissolution of 1.8 mg of **1** in 400 μL of a D_2O solution of $H_3Sb_3P_2O_{14}$ at 3% w/w (final concentration of the sugar: 8.3 mM). In each case, the monitoring of the ^2H NMR signal of D_2O was used to check the orientation of the liquid crystal through the quadrupolar splitting.

5.2.2. ^1H and ^{13}C assignment. All NMR spectra were acquired at 293 K on Bruker spectrometers operating at 500, 600 or 800 MHz ^1H-Larmor frequency, equipped with 5 mm inverse triple resonance probeheads with three axes gradients. The ^1H and ^{13}C NMR spectra were assigned at 293 K using classical 2D experiments, leading to chemical shifts (Tables 3 and 4) in agreement with those of similar compounds.[31,32,35,37]

5.2.3. Residual dipolar couplings. The RDCs were extracted by measuring the frequency splittings in the proton dimension of HSQC experiments with sensitivity enhanced by gradients.[39] These experiments were performed on a Bruker DRX800 spectrometer for **2**, and on Bruker DRX500 and DRX600 spectrometers for **1**. The RDC values were obtained using a modification of a program, written in C and Tcl/Tk languages, devoted to the measurement of homonuclear scalar coupling constants in COSY spectra,[47] employing frequency domain deconvolution.[48] Our modified version was designed for the measurement of heteronuclear one-bond coupling constants and rendered easy the comparison of values taken from two spectral sources.

5.2.4. Proton–proton distance determination. For **1**, 19 internuclear distances (2 ambiguous) were extracted from an off-resonance ROESY build-up curve comprising five different mixing times, at an angle $\vartheta = 54.7^\circ$ between the static and effective magnetic field in the rotating frame.[49] Seven out of the 19 distances corresponded to inter-unit interactions (Table 5).

For **2**, the proton–proton distances were determined via the procedure described by Desvaux and coworkers.[50] Briefly, 4 NOESY and 16 off-resonance ROESY spectra were acquired using 256×2048 real points on a Bruker DRX 500 spectrometer. The overall set of experiments corresponded to four different mixing times and five angles ϑ ranging from 0 to 54.7°. All non overlapped diagonal- and cross-peaks were integrated and processed using a home-written C program. In a first step, the cross-relaxation rates σ_{ij}^{ϑ} were determined at a given angle ϑ by a linear least-square fitting of the build-up curve. Then for each pair of spins, the five extracted rates were fitted to the theoretical equation:

$$\sigma_{ij}^{\vartheta} = \cos^2 \vartheta \, \sigma_{ij}^{0^\circ} + \sin^2 \vartheta \, \sigma_{ij}^{90^\circ}. \quad (7)$$

in order to determine the longitudinal $\sigma_{ij}^{0^\circ}$ and transverse $\sigma_{ij}^{90^\circ}$ cross-relaxation rates. Assuming a Lorentzian spectral density function for each pair of spins, these

Table 3
^{1}H and ^{13}C chemical shifts at 293 K and one-bond ^{1}H–^{13}C residual dipolar couplings (RDC) measured in aqueous suspensions of V_2O_5 and $H_3Sb_3P_2O_{14}$ for the trisaccharide **1**

Unit	C–H Pair	δ ^{1}H	δ ^{13}C	RDC V_2O_5	RDC $H_3Sb_3P_2O_{14}$
Gal	1	4.590	98.78	8.9*	1.2*
Gal	2	3.634	67.98	16.0	18.0
Gal	3	3.791	69.44	9.4	17.1
Gal	4	4.034	65.34	48.0	−39.8
Gal	5	3.740	71.81	−5.0*	10.4*
Fuc	1	5.242	95.62	21.8	−38.7
Fuc	2	3.821	64.65	−2.3	5.7
Fuc	3	4.041	66.21	9.7	5.4
Fuc	4	3.931	68.88	19.9	−34.9
Fuc	5	4.984	63.65	−1.9*	4.8*
GlcNAc	1	4.606	98.68	36.6*	1.2*
GlcNAc	2	4.050	52.61	64.4	0.4
GlcNAc	3	3.991	71.98	44.0*	−7.2*
GlcNAc	4	4.075	70.34	65.8	−2.9
GlcNAc	5	3.732	72.24	56.3	−2.8*

The RDC values followed by * are measured with a lower accuracy mainly due to overlap of at least one of the two peaks. The ^{1}H chemical shift of the HDO peak is taken at 4.93 ppm as a reference, the ^{13}C chemical shifts are not referenced and are only indicative.

Table 4
^{1}H and ^{13}C chemical shifts and one-bond ^{1}H–^{13}C residual dipolar couplings (RDC) measured in aqueous suspensions of V_2O_5 and $H_3Sb_3P_2O_{14}$ for the pentasaccharide **2**

Unit	C–H Pair	δ ^{1}H	δ ^{13}C	RDC V_2O_5	RDC $H_3Sb_3P_2O_{14}$
Gal	1	4.605	98.33	−3.5*	−0.5*
Gal	2	3.651	66.07	−1.0	−5.0
Gal	3	4.344	77.14	−4.4	−4.5
Gal	4	4.290	63.28	7.7	−4.6
Gal	5	3.687	71.60	−4.4	−3.6
Fuc	1	5.157	95.54	5.4	3.6
Fuc	2	3.707	64.65	2.4	−6.0
Fuc	3	3.932	66.14	2.2	−6.7
Fuc	4	3.809	68.85	6.6	1.9
Fuc	5	4.949	63.65	1.9	−6.5
GlcNAc	1	4.727	99.59	13.6	−5.8
GlcNAc	2	3.999	52.92	13.6*	−6.9*
GlcNAc	3	3.897	71.55	12.4*	−3.2*
GlcNAc	4	4.017	70.06	14.0	−5.2
GlcNAc	5	3.608	71.90	12.7*	−3.8*
Gal	1	4.451	99.89	9.6	−2.4
Gal	2	3.591	66.99	10.1	0.6
Gal	3	3.733	79.08	10.1	4.3
Gal	4	4.186	65.26	0.3	0.2
Gal	5	3.728	71.84	9.7*	−1.1*
Glc	1	4.429	100.0	6.6	−1.6
Glc	2	3.322	69.72	4.6	−2.1
Glc	3	3.662	75.23	8.2	−1.3
Glc	4	3.629	71.70	6.5	−0.2
Glc	5	3.659	71.31	7.7	0.2

The RDC values followed by * correspond to values with a lower accuracy mainly due to peak overlap. The ^{1}H chemical shift of the HDO peak is taken at 4.93 ppm as a reference, the ^{13}C chemical shifts are not referenced and are only indicative.

Table 5
Inter-proton distances in Å as extracted from off-resonance ROESY build-up curves for the trisaccharide **1**

Unit	Proton	Unit	Proton	Distance	Unit	Proton	Unit	Proton	Distance
Gal	1	Gal	2	2.6	Gal	1	Gal	3	2.6
Gal	1	GalNAc	4	2.5	Gal	1	GalNAc	3,6′	2.4
Gal	1	GalNAc	6	2.8	Fuc	1	Fuc	2	2.3
Fuc	1	Fuc,GalNAc	3,2	2.5	Fuc	5	Fuc	3	2.3
Fuc	5	Fuc	4	2.3	Fuc	1	GalNAc	3	2.3
Fuc	5	Gal	2	2.4	GalNAc	1	GalNAc	2	2.7
Nag	1	GalNAc	3	2.5	GalNAc	1	GalNAc	5	2.3
Nag	1	GalNAc	Me	2.9	GalNAc	6	GalNAc	6′	1.8
Nag	6	GalNAc	5	2.4					

two rates were converted into an internuclear distance r_{ij} and a correlation time per pair of proton τ_{cij}. With this procedure, 48 internuclear distances (6 ambiguous) were obtained for **2**. Fifteen of them corresponded to inter-unit interactions (Table 6).

5.3. Molecular modelling

5.3.1. Structure of the oligosaccharides from NOE data. The same protocol has been used for **1** and **2**. The proton–proton distances extracted from the off-resonance ROESY experiments were used in a simulated annealing procedure using the XPLOR 3.1 software.[51] The error bars on the distances were derived from least square fitting of the cross-relaxation rates; most of them were equal to ± 0.2 Å. Starting from a template structure with reasonable geometry, a simulated annealing with a high temperature dynamics step of 1000 K during 35 ps with a timestep of 3.5 fs was performed. During this dynamics, low weight on the van der Waals terms and progressive increase of the weight of the NOE terms insured good sampling of the conformational space. A slow cooling of 28 ps followed in order to restore the usual values of the covalent energy terms. This procedure was repeated 50 times, resulting in 50 structures which were accepted or rejected following criteria based on the geometry and NOE violations.

5.3.2. Energy maps for the glycosidic bonds. Energy-relaxed ϕ/ψ maps for the glycosidic linkages were computed *in vacuo* with the InsightII/DISCOVER program[52] using the CFF91 force field.[53] For each

Table 6
Inter-proton distances in Å as extracted from off-resonance ROESY build-up curves for the pentasaccharide **2**

Unit	Proton	Unit	Proton	Distance	Unit	Proton	Unit	Proton	Distance
Gal	1	Gal	3	2.6	Gal	1	Gal	5	2.3
Gal	1	Gal	6,6′	3.4	Gal	1	GalNAc	2,4	2.3
Gal	1	GalNAc	6′	2.5	Gal	2	Gal	3	3.2
Gal	3	Gal	4	2.6	Gal	3	Gal	5	2.6
Gal	3	Gal	6,6′	3.5	Gal	4	Gal	5	2.5
Gal	4	Gal	6,6′	2.8	Fuc	1	Fuc	2	2.5
Fuc	1	GalNAc	2	3.2	Fuc	1	GalNAc	3	2.6
Fuc	3	Fuc	2	3.5	Fuc	3	Fuc	4	2.6
Fuc	3	GalNAc	6	3.0	Fuc	5	Gal	2	2.9
Fuc	3	Fuc	5	2.8	Fuc	4	Fuc	5	2.9
Fuc	5	GalNAc	4	4.1	Fuc	6*	Gal	2	3.0
Fuc	6*	Fuc	4	3.1	GalNAc	1	GalNAc	2	3.1
GalNAc	1	GalNAc	3	2.8	GalNAc	1	Gal-4	2	2.3
GalNAc	1	Gal-4	3	2.2	GalNAc	1	Gal-4	4	3.3
GalNAc	6	Nag	5	2.8	GalNAc	6′	GalNAc	5	2.8
Gal-d	1	Gal-d	5	2.4	Gal-d	1	Gal-d	6	3.1
Gal-d	1	Glc	5	2.2	Gal-d	1	Glc	6	3.4
Gal-d	4	Gal-d	6	2.6	Gal-d	4	Gal-d	3	2.2
Glc	1	Glc	5	2.1	Glc	1	Glc	2	3.4
Glc	6	Glc	6′	2.1	Glc	6	Glc	3	2.9
Glc	2	Glc	3,5	2.6	Glc	6	Glc	3,5	2.8

map, the simulation conditions were the following: the dihedral angles were varied using 10° steps and 2000 cycles of conjugated gradient served for the minimization; a scalar dielectric constant of 80 was used. The glycosidic dihedral angles were restrained by a potential with a force constant of 500 kcal rad^{-2} mol^{-1}.

5.3.3. Structure of the oligosaccharides from RDC. The structures of the oligosaccharides based solely on RDCs were obtained using an home-written C program, whose efficiency was first checked on simulated data. The key elements of this program designed to define the oligosaccharide structure were the following:

1) For each pyranose unit, an attached frame (Fig. 2) was defined with the OZ axis parallel to the C-1–O-1 bond and the OY axis defined by the direct product $\overrightarrow{\text{C-1–O-1}} \wedge \overrightarrow{\text{C-1–H-1}}$ (we denoted such frame {C-1, H-1, O-1}). The directions of all C–H bonds of a pyranose unit were defined in this frame.
2) The orientation of one pyranose ring with respect to the next one was computed using an intermediate frame defined on the second carbon involved in the glycosidic bond. For instance, the computation of the orientation of the sulfated galactopyranose unit (a) relative to the glucosamine unit (c) consisted in performing the change of frame from {Gal(a) C-1, Gal(a) H-1, GlcNAc O-4} to {GlcNAc C-4, GlcNAc H-4, GlcNAc O-4}, and then to {GlcNAc C-1, GlcNAc H-1, GlcNAc O-1}. The pyranose ring being rigid, the two degrees of freedom to be adjusted in this example were the α and γ values of the first set of Euler angles. They corresponded to the two rotation angles along the Gal(a) C-1–GlcNAc O-4 bond and along the GlcNAc C-4–GlcNAc O-4 bond (Fig. 2), and were consequently associated to the torsion angles ϕ and ψ defining this glycosidic bond. According to energy-minimized structures, one found:

$$\psi = \alpha - 60.5^\circ \quad (8)$$

$$\phi = 244.3^\circ - \gamma \quad (9)$$

Similar relations could be used for all glycosidic bonds.
3) The frame of the fucose unit was linked to the frame where the alignment tensor is diagonal by three Euler angles (α_R, β_R, γ_R). Assuming the presence of a rhombocity, due to the symmetry properties of Wigner matrices in Eq 5, we noted that:

$$\alpha_R \in [0,\ 90^\circ],\ \ \beta_R \in [0,\ 90^\circ]. \quad (10)$$

Using this range of values, D_r might take negative values. Changing the sign of D_r/D_a was performed by transforming α into $\alpha + 90^\circ$. By restricting the search domain of this set of Euler angles, the problem of degeneracy of dipolar couplings which required the need of, at least, two independent media,[18] disappeared.

The geometry of the oligosaccharide being defined in such a way and for a given set of α_R, β_R and γ_R values, for each (C,H) pair the program computed the two coefficients composed of products of Wigner matrices in Eq 5 each being multiplied either by D_a or D_r. This set of 15 pairs of coefficients allowed one to determine by linear least-square fitting the D_a and D_r values to the experimental RDC, a figure of merit through the resulting χ^2 value and the consistence of the result through the relation $|D_r/D_a| < \sqrt{1/6}$.[24]

The determination of the best set of angles (ϕ, ψ, α_R, ...) was performed thanks to a grid search based on the χ^2 values. In order to speed up this search protocol, a minimizing procedure based on the Simplex algorithm[54] was finally applied to optimize the set of angles. According to the position in the full algorithm (Fig. 5), the set of angles were constituted by either the four glycosidic angles (ϕ, ψ) or the angles defining the molecular frame (α_R, β_R, γ_R) for the Section 2.4.1 (procedure **a**) or by all angles (ϕ, ψ, α_R, β_R, γ_R) for the Section 2.4.2 (procedure **b**).

5.3.4. Calculation of the orientation of the Gal (d) unit. When a part of the structure is defined, it becomes possible to compute the orientation of the next unit relative to the previous ones. For instance, considering the orientation of the Gal (d) unit of the pentasaccharide relative to the Lewis^x motif, we have used fixed parameters (D_a, D_r, α_R, β_R, γ_R) for the RDC tensor as calculated (in Section 2.4.1), and we have tried to optimize the two glycosidic angles of GlcNAc/Gal(d) (Fig. 7). The problems encountered with the RDC and the influence of the flexibility of this glycosidic link on the RDCs certainly explain why the RDC-based results differ so strongly from those obtained by the off-resonance ROESY approach which takes into account internal mobility. However, two features can be noted. Firstly, the minima found with RDCs measured in aqueous suspensions of V_2O_5 and $H_3Sb_3P_2O_{14}$ now strongly differ, while they are only slightly incompatible in the case of the Lewis^x motif (Table 2). This remark raises the question on combining RDC measured in different media for medium-size molecules. Secondly, this example shows the robustness of our approach using internal degrees of freedom, since the fourfold degeneracy is not encountered. This problem would appear if we had tried to orient this pyranose unit relative to the Lewis^x motif by working directly with rigid independent elements referred to the orientation of the RDC tensor.

Acknowledgements

The synthesis of the two saccharides[46] was performed by Y. M. Zhang and P. Sinaÿ, that we acknowledge for providing us these products. Patrick Davidson and Maurice Goldman are greatly acknowledged for their helpful comments. The 'Association pour la Recherche contre le Cancer' is acknowledged for financial support (Grant #4524). The 800 MHz NMR spectrometer at Gif sur Yvette was financed with the help of the 'Région Ile de France' and the 'Association pour la Recherche contre le Cancer'. FAS acknowledges Region Ile de France and Bruker Biospin for a Ph.D. fellowship.

References

1. Bax, A.; Kontaxis, G.; Tjandra, N. *Methods Enzymol.* **2001**, *339*, 127–174.
2. Prestegard, J. H.; Valafar, H.; Glushka, J.; Tian, F. *Biochemistry* **2001**, *40*, 8677–8685.
3. Aroulanda, C.; Merlet, D.; Courtieu, J.; Lesot, P. *J. Am. Chem. Soc.* **2002**, *124*, 12059–12066.
4. Schwalbe, H.; Grimshaw, S. B.; Spencer, A.; Buck, M.; Boyd, J.; Dobson, C. H.; Redfield, C.; Smith, L. J. *Protein Sci.* **2001**, *10*, 677–688.
5. Kiddle, G. R.; Homans, S. W. *FEBS Lett.* **1998**, *436*, 128–130.
6. Rundlöf, T.; Landersjö, C.; Lycknert, K.; Maliniak, A.; Widmalm, G. *Magn. Reson. Chem.* **1998**, *36*, 773–776.
7. Neubauer, H.; Meiler, J.; Peti, W.; Griesinger, C. *Helv. Chim. Acta* **2001**, *84*, 243–258.
8. Martin-Pastor, M.; Bush, C. A. *Carbohydr. Res.* **2000**, *323*, 147–155.
9. Gabriel, J.-C. P.; Davidson, P. *Adv. Mater.* **2000**, *12*, 9–19.
10. Desvaux, H.; Gabriel, J.-C. Y.; Berthault, P.; Camerel, F. *Angew. Chem.* **2001**, *40*, 373–376.
11. Livage, J. *Chem. Mater.* **1991**, *3*, 578–593.
12. Gabriel, J.-C. P.; Camerel, F.; Lemaire, B. J.; Desvaux, H.; Davidson, P.; Batail, P. *Nature* **2001**, *413*, 504–508.
13. Cai, M.; Huang, Y.; Zheng, R.; Wei, S.-Q.; Ghirlando, R.; Lee, M. S.; Craigie, R.; Gronenborn, A. M.; Clore, G. M. *Nat. Struct. Biol.* **1998**, *5*, 903–909.
14. Skrynnikov, N. R.; Goto, N. K.; Yang, D.; Choy, W.-Y.; Tolman, J. R.; Müller, G. A.; Kay, L. E. *J. Mol. Biol.* **2000**, *295*, 1265–1273.
15. Clore, G. M. *Proc. Natl. Acad. Sci. USA* **2000**, *97*, 9021–9025.
16. Martin-Pastor, M.; Bush, C. A. *Biochemistry* **2000**, *39*, 4674–4683.
17. Tian, F.; Al-Hashimi, H. M.; Craighead, J. L.; Prestegard, J. H. *J. Am. Chem. Soc.* **2001**, *123*, 485–492.
18. Ramirez, B. E.; Bax, A. *J. Am. Chem. Soc.* **1998**, *120*, 9106–9107.
19. Hajduk, P. J.; Horita, D. A.; Lerner, L. E. *J. Am. Chem. Soc.* **1993**, *115*, 9196–9201.
20. Rose, M. E. *Elementary Theory of Angular Momentum*; John Wiley & Sons: New York, 1963.
21. IUPAC *Pure Appl. Chem.*, **1983**, *55*, p. 1269.
22. Veracini, C. In *NMR of Liquid Crystals*; Emsley, J. W., Ed.; D. Reidel Publishing Company: Dordrecht, 1985; pp 99–122.
23. Tjandra, N.; Bax, A. *Science* **1997**, *278*, 1111–1114.
24. Clore, G. M.; Gronenborn, A. M.; Bax, A. *J. Magn. Reson.* **1998**, *133*, 216–221.
25. Moltke, S.; Grzesiek, S. *J. Biomol. NMR* **1999**, *15*, 77–82.
26. Zannoni, C. In *NMR of Liquid Crystals*; Emsley, J. W., Ed.; D. Reidel Publishing Company: Dordrecht, 1985; pp 35–52.
27. Desvaux, H.; Berthault, P.; Birlirakis, N.; Goldman, M. *J. Magn. Reson.* **1994**, *A108*, 219–229.
28. Desvaux, H.; Berthault, P. *Prog. NMR Spectrosc.* **1999**, *35*, 295–340.
29. Berthault, P.; Birlirakis, N.; Rubinstenn, G.; Sinaÿ, P.; Desvaux, H. *J. Biomol. NMR* **1996**, *8*, 23–35.
30. Lin, Y.-C.; Hummel, W.; Huang, D.-H.; Ichikawa, Y.; Nicolaou, K. C.; Wong, C.-Y. *J. Am. Chem. Soc.* **1992**, *114*, 5452–5454.
31. Miller, K. E.; Mukhopadhyay, C.; Cagas, P.; Bush, C. A. *Biochemistry* **1992**, *31*, 6703–6709.
32. Mukhopadhyay, C.; Miller, K. E.; Bush, C. A. *Biopolymers* **1994**, *34*, 21–29.
33. Perez, S.; Mouhous-Riou, N.; Nifant'ev, N. E.; Tsvetkov, Y. E.; Bachet, B.; Imberty, A. *Glycobiology* **1996**, *6*, 537–542.
34. Yvelin, F.; Zhang, Y.-M.; Mallet, J.-M.; Robert, F.; Jeannin, Y.; Sinaÿ, P. *Carbohydr. Lett.* **1996**, *1*, 475–482.
35. Henry, B.; Desvaux, H.; Pristchepa, M.; Berthault, P.; Zhang, Y. M.; Mallet, J.-M.; Esnault, J.; Sinaÿ, P. *Carbohydr. Res.* **1999**, *315*, 48–62.
36. Imberty, A.; Perez, S. *Chem. Rev.* **2000**, *100*, 4567–4588.
37. Zhang, Y. M.; Dausse, B.; Sinaÿ, P.; Afsahi, M.; Desvaux, H.; Berthault, P. *Carbohydr. Res.* **2000**, *324*, 231–234.
38. Pelletier, O.; Sotta, P.; Davidson, P. *J. Phys. Chem. Sect. B* **1999**, *103*, 5427–5433.
39. Kay, L. E.; Keifer, P.; Saarinen, T. *J. Am. Chem. Soc.* **1992**, *114*, 10663–10665.
40. Ottiger, M.; Delaglio, F.; Bax, A. *J. Magn. Reson.* **1998**, *131*, 373–378.
41. Brutscher, B. *J. Magn. Reson.* **2001**, *151*, 332–338.
42. Goldman, M. *J. Magn. Reson.* **1984**, *60*, 437–452.
43. Tjandra, N.; Bax, A. *J. Magn. Reson.* **1997**, *124*, 512–515.
44. Tjandra, N.; Grzesiek, S.; Bax, A. *J. Am. Chem. Soc.* **1996**, *118*, 6264–6272.
45. Weiss, G. H.; Ferreti, J. A.; Kiefer, J. E. *J. Magn. Reson.* **1982**, *46*, 69–83.
46. Zhang, Y.M.; Sinaÿ, P. *Carbohydr. Res.*, this issue, see following communication: doi:10.1016/S0008-6215(03)00242-8.
47. Jeannerat, D. *Magn. Reson. Chem.* **2000**, *38*, 156–164.
48. Jeannerat, D.; Bodenhausen, G. *J. Magn. Reson.* **1999**, *141*, 133–140.
49. Desvaux, H.; Berthault, P.; Birlirakis, N.; Goldman, M.; Piotto, M. *J. Magn. Reson.* **1995**, *A113*, 47–52.

50. Desvaux, H.; Berthault, P.; Birlirakis, N. *Chem. Phys. Lett.* **1995**, *233*, 545–549.
51. Brünger, A. T. *X-PLOR Version 3.1, A System for X-ray Crystallography and NMR*; Yale University Press: New Haven, 1992.
52. BIOSYM/MSI, Vol. 9685, Scranton Road, San Diego, CA92121-3752.
53. Maple, J. R.; Hwang, M. J.; Stockfish, T. P.; Dinur, U.; Woldman, M.; Ewig, C. S.; Hagler, A. T. *J. Comput. Chem.* **1994**, *15*, 162–182.
54. Press, W. H.; Teukolsky, S. A.; Vetterling, W. T.; Flannery, B. P. *Numerical Recipes in C. The Art of Scientific Programming*; Cambridge University Press: Cambridge, 1988.